COBEM 2021 26th International Congress of Mechanical Engineering
ABCM Associação Brasileira de Engenharia e Ciências Mecânicas
November 22-26, 2021, Virtual Congress, Brazil

COB-2021-1141
FLOW DYNAMICS AND AERODYNAMIC FORCES ON AN ADAPTED AHMED BODY AT MODERATE REYNOLDS NUMBERS THROUGH NUMERICAL SIMULATION

Marcos Heduardo Pereira da Silva
Raul Victor Teixeira Rosseto
Fernando Augusto Alves Mendes
Augusto Salomão Bornschlegell
UFGD, FAEN, Rodovia Dourados – Itahum, Km 12 – Cidade Universitária, Cx. Postal 364 – CEP 79804-970
marcos_heduardo@hotmail.com, raul07_rosseto@hotmail.com, fernandomendes@ufgd.edu.br, augustosalomao@ufgd.edu.br

Abstract. *In this work, we evaluate the flow dynamics around an adapted Ahmed's body and its implications on aerodynamic forces. A fillet between the top surface and the rear chanfer is added to the original Ahmed body benchmark considering the original chanfer angle of 30°. Different fillet radius and inlet velocities were evaluated, so that Reynolds Numbers ranged from 4.8 x* 10^3 *to 4.8 x* 10^4*. In order to predict the flow behavior and the aerodynamic forces, a numerical model was built in the OpenFOAM environment, considering a transient, bidimensional, incompressible and isothermal flow model with constant properties. The advective terms were modeled using a second order Upwind scheme and the time integration was performed using a second order backward scheme. PISO algorithm was used to solve the pressure-velocity coupling by the pisoFoam solver and the modeled physical time was 2 seconds. The initial flow condition was the solution of the equivalent steady state problem using the simpleFoam solver. It was observed in the results that the models with smaller radius for the highest velocities have the smallest drag coefficients in relation to the larger radius. The models with larger radius for the smallest velocities have the smallest drag coefficients in relation to the smaller radius.*

Keywords: *Ahmed body, Aerodynamics, Turbulence, OpenFOAM, Open source*

1. INTRODUCTION

Conducting aerodynamics studies on land vehicles is of great value, as it is possible to reach increasingly better points in relationship to land transport efficiency, which is the key point for reducing fuel consumption and increasing its useful life and safety. One of its main fundamentals is aerodynamic drag, which can be defined as a force contrary to the movement of a body immersed in fluid. Another factor that can be evaluated is the flow around the bluff bodies, where the flow is dominated by large regions of separate flow, which until today causes great challenges to the engineering design.

Castejo (2011) carried out an aerodynamic study on a basic geometry, which represents similarity to hatchback vehicles, called the SAE Model in a computational environment. The concepts of vehicle drag and vehicle stability were exposed to support this study, where it was shown that drag and vehicle stability comprise different concepts, which can decrease the drag of a vehicle without loss of stability. Aerodynamic drag is the key to vehicle efficiency.

Increasingly looking to reduce costs, time and losses in the development of projects in a variety of fields, industries are considerably increasing the flow of computational solutions, testing the most diverse types of settings, using the experimental methodology only for numerical validation. The tendency in the industry is to invest massively in computational solutions, testing countless hypotheses and configurations, using experiments only for the final decision of a project or testing the chosen solution, or even for the validation of numerical models (Carregari, 2006).

To carry out numerical studies, comparing with experimental ones, there are several models in the literature. A highly used model was proposed by Ahmed *et al.* (1984). It is a benchmark model of relevant importance for the automotive industry and it is a reference for studies of vehicle aerodynamics and wind tunnel calibration. This model is a simplified automobile to perform aerodynamic studies. The geometry (Figure 1) of Ahmed body tends to have the essential features of a land vehicle, except for flow in the engine compartment, trunk and passengers, rotation of the wheels, mirrors and weather conditions as water, mud and dust in the lower part of the vehicle. This model is characterized by an elongated body, front face with rounded edges, slope at the rear at a specific angle (α) which is widely studied. This variation in the rear angle allows to obtain vortex structures at the rear of the model, responsible for most of the drag.

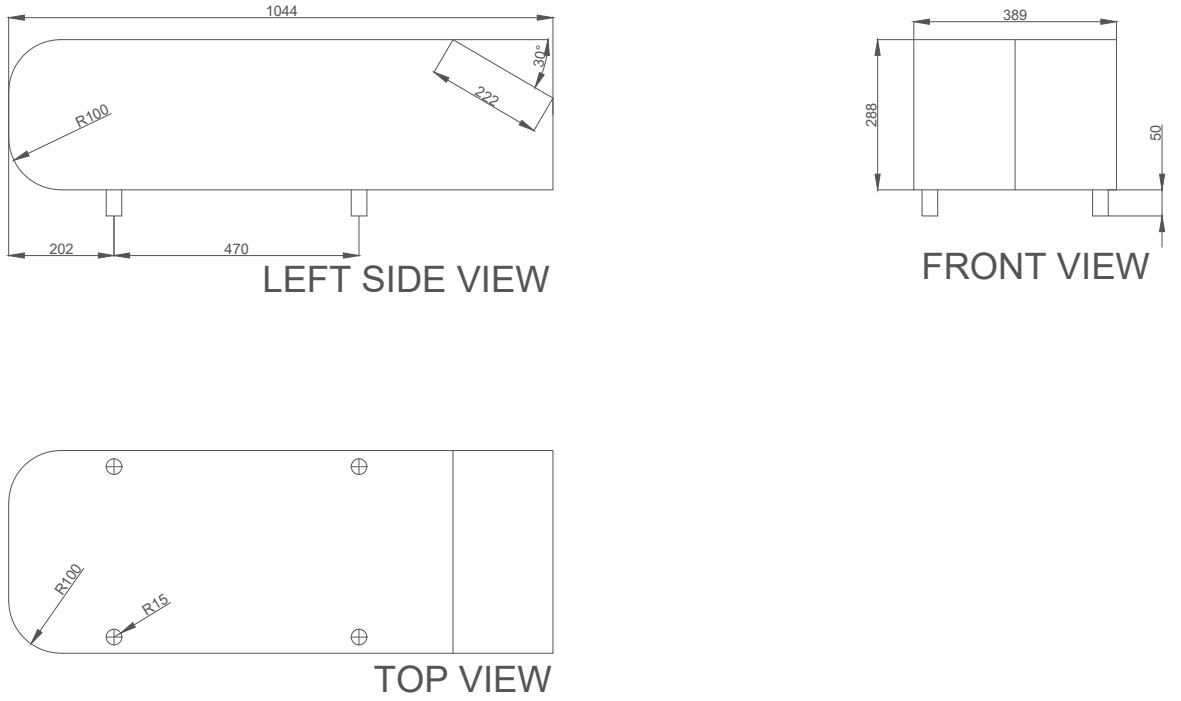

Figure 1. Ahmed Body

For the computational analysis of a model (buff and slim), the most different types of software for Computational Fluid Dynamics (CFD) are commonly used, with the feature of practicality, reliability in the results obtained, speed and for being more economically viable compared to the experimental method. For the conclusion of any numerical study, it is necessary to understand the project requirements, knowledge of the numerical methods employed and the numerical tool (software) to be used and a computational processing compatible with the degree of complexity of the project.

The experimental study aims to validate the computational analysis, usually tested in a wind tunnel. In this analysis it is possible to directly observe the influence in different flow situations around the model, where several factors can be analyzed, such as drag and lift force, vortex frequency, body behavior in relation to the soil, always looking for reproduction with the reality with the different sectors where they are used, such as aerospace, automobile, oil, naval, civil, among others. It is common to say that the experimental and numerical analysis is not canceled, but one complements the other, thus generating increasingly elaborate projects.

Rocha (2016) performed the numerical analysis using commercial software Ansys for CFD of the external flow field, using Ahmed's geometry as a reference. The purpose of this study was to obtain drag and pressure forces and compare them with the results obtained by Raina *et al.* (2017). Different angles were used in the upper rear chamfer from 0° to 60°. It was observed that at angles of 20° to 40° they have higher lift coefficients. The presence of vortex directly affects the drag coefficient, where it reduces considerably when the angle changes from 30° to 35°. The greater the angle, the lower the drag coefficient.

Ataídes (2009) performed the experimental analysis, using the effects of non linearity on the Reynolds tensor in turbulence models, around Ahmed's body. The results obtained were the pressure coefficient on the surface, transversal profiles of medium speed and turbulent kinetic energy. The results obtained were compared with the literature, where they were validated for having a great correlation.

Sousa *et al.* (2010) performed the numerical and experimental analysis of the flow around a road vehicle (bus), where the numerical analysis was performed using the CFD technique and the experimental one using a wind tunnel. The purpose of the project employed was to increase aerodynamic efficiency. The main point studied was the variation in the drag coefficient due to the variation in the yaw angle (α), located at the rear of the body. The numerical and experimental results were validated, where the values were practically the same. Results were also presented for pressure fields, velocity, velocity vectors, vorticity, current lines, in addition to the behavior of the boundary layer. Comparisons with experimental solutions were also presented. The values for the drag coefficients obtained were close to the values obtained in tests carried out in wind tunnels.

The present work evaluates, by numerical simulation, at Reynolds Numbers ranging from 4.80 x 10^3 to 4.80 x 10^4, the flow past the Ahmed body with geometrical modification considering the relative motion between the Ahmed body and the ground. The geometrical modification consists in the addition of a fillet between the top surface and the rear chamfer. Six fillet radius will be evaluated for four different velocities in order to predict the flow behavior and the related

aerodynamic forces.

2. METODOLOGY

For the numerical solution of the flow past the Ahmed body and the study of aerodynamic forces, the open access software, OpenFOAM 7.0 with the pisoFoam solver was used. For the preparation of the geometrical model, the open source program, FreeCAD, was used. Different fillets were adapted between the top surface and the rear chamfer, considering a slant angle of 30° for all cases. Seven different fillet types were studied for 4 velocities, totaling 28 cases, including the original benchmark case. For the fillets, radius 0.005 (R05), 0.0010 (R10), 0.0015 (R15), 0.0020 (R20), 0.0050 (R50), 0.0075 (R75) m and Ahmed's original body were used. The fillet geometry is created by imposing the tangent mating condition in both edges and the filet radius magnitude.

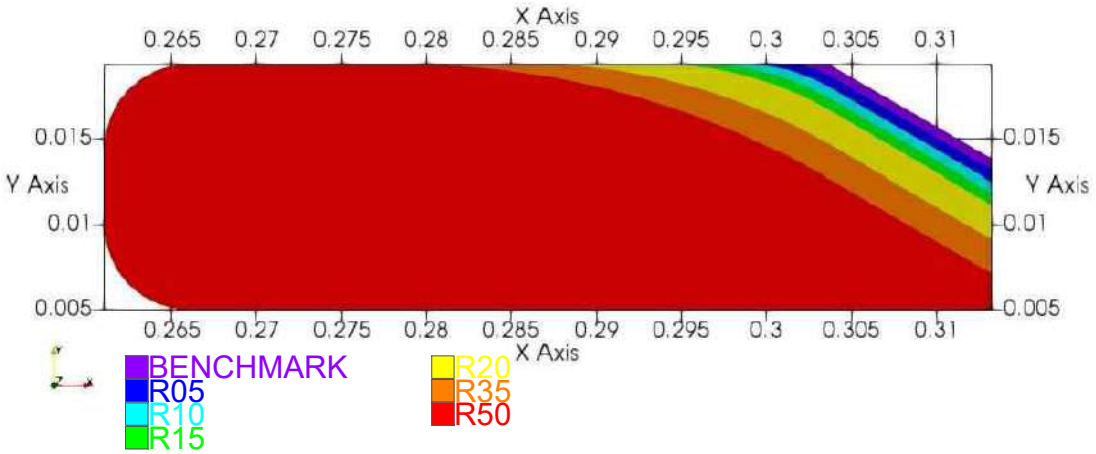

Figure 2. Studyed models

The final mesh was created using snappyHexMesh solver. The mesh was extruded perpendicular to the xy plane, where the z-axis extrusion creates a three-dimensional mesh. For the initial mesh creation using blockMesh, the mesh geometric parameter used was the length of the Ahmed body L and its height h. The numerical domain has 5 times L upstream, 15 times L downstream, 10 times h to the upper limit and 0.1 times h for the lower limit as illustrated in Figure 2. The extrusion length (perpendicular) was 0.05 times L. This domain setup was based on previous works, such as Krajnovic and Davidson (2005) and Guilmineau *et al.* (2018). The resulting mesh is composed of 3843548 hexahedral cells, being three-dimensional. In despite of the three-dimensional nature of the flow, due computational processing limitations, the elements were extruded in the direction perpendicular to the plane in only one volume, thus creating a lighter 2D model with 346202 cells. We performed a mesh sensibility analysis by increasing the mesh refinement in one level at the snappyHexMesh utility, that is, the smallest cell dimension at the finer mesh was half of the smallest cell in the coarser one. The resulting finer mesh had 833880 cells. In the finer mesh, the obtained drag coefficient was 4% lower than the coarser mesh. Due the computational limitations, such as hard disk and ram memory, we used the mesh with 346202 cells.

The simpleFoam solver was used to obtain the steady state solution which is used as initial condition for the pisoFoam, the transient solver used to generate the final data exploited in the present work. In the transient model, the simulated total physical time is 2 seconds. A kinematic viscosity of 1 x 10^5 m²/s was considered. Thus, a transient, two-dimensional, incompressible and isothermal model with constant properties was considered. The boundary conditions were prescribed velocity at the inlet, zero gradient implementation that allows reverse flow at the outlet, slip condition at the top boundary and moving wall boundary condition at bottom, at the same inlet velocity, so that the relative motion between the ground and the Ahmed body could be represented. Velocities of 5 (V05), 10 (V10), 20 (V20) and 50 (V50) m/s were used. Four inlet velocities, and then, four Reynolds Numbers (cases) were evaluated: Re_A = 4.80 x 10^3 (5 m/s), Re_B = 9.60 x 10^4 (10 m/s), Re_C = 1.92 x 10^4 (20 m/s) and Re_D = 4.80 x 10^4 (50 m/s).

Regarding the numerical methods, the standard OpenFOAM K-omega SST turbulence model (Menter *et al.*, 2003) was used with a turbulent intensity of 3%. Both turbulence model and intensity were arbitrated. The defined time integration scheme was the backward second order type. The advective terms were modeled using a second order Upwind scheme. For the diffusive terms, the central differences scheme was employed. To setup the model, the Courant number was fixed in 1 and the variable time step was used.

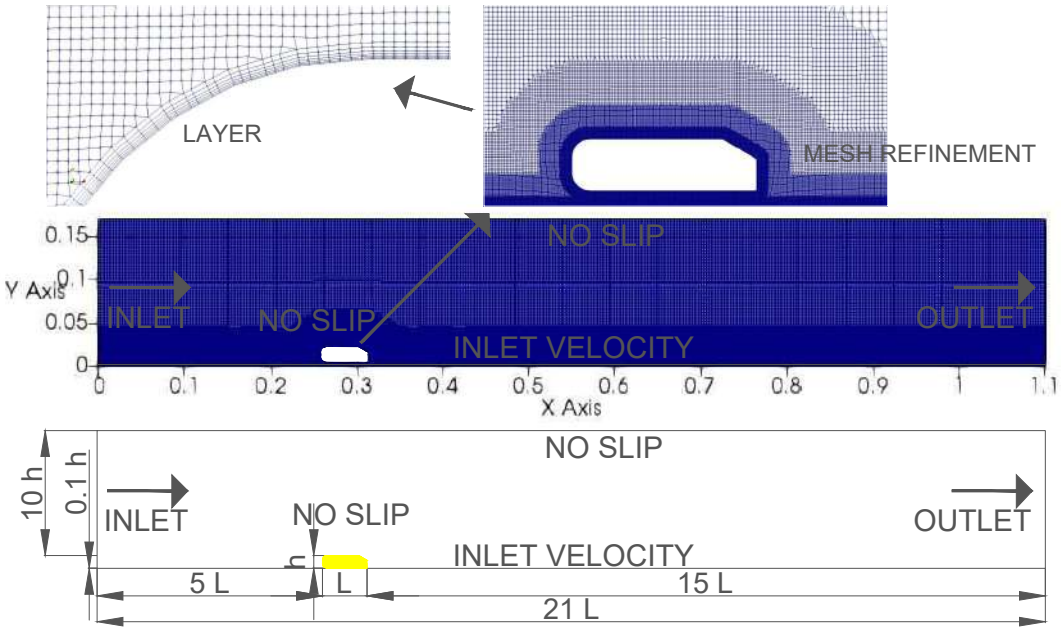

Figure 3. Boundary conditions

2.1 EQUATIONS

For the numerical solution in this work (using the pisoFoam), the calculations of the parameters to be used as boundary conditions were performed. Thus, defining the Reynolds Number obtained by Eq. 1, the turbulent kinetic energy obtained by Eq. 2, at turbulent dissipation rate, obtained by Eq. 3, at specific turbulent dissipation rate, obtained by Eq. 4.

$$Re = \frac{\rho \cdot V \cdot H}{\mu} \tag{1}$$

Where Re = Reynolds Number, dimensionless parameter that defines the flow (laminar, transition or turbulent). ρ = stands for the air density $(kg.m^3)$. V = Velocity (m/s), input velocity considered in the boundary conditions. H = height (m). μ = stands for the air viscosity $(Pa.s)$.

$$K_t = \frac{3}{2}\left(\frac{V \cdot I}{100}\right)^2 \tag{2}$$

Where K_t = Turbulent kinetic energy $(\frac{m^2}{s^2})$, kinetic energy calculated from the input velocity. I = turbulent intensity $(\%)$.

$$\epsilon = \frac{C_\mu \cdot K_t^{\frac{3}{2}}}{L'} \tag{3}$$

Where ϵ = turbulent dissipation rate $(\frac{m^2}{s^2})$, C_μ = is a turbulence model constant, L' = turbulence length (m).

$$\omega = \frac{\sqrt{K_t}}{L'} \tag{4}$$

Where ω = specific turbulent dissipation rate $(\frac{1}{s})$.
Finally, the drag and lift coefficients are defined by the equation below (Eq. 6):

$$C_{D,L} = \frac{2 \cdot F_{D,L}}{\rho \cdot A \cdot V^2} \tag{5}$$

Where: $C_{D,L}$ = Drag coefficient and body support $(dimensionless)$, $F_{D,L}$ = Drag force and lift (N), A = Frontal area (m^2), in this work the Ahmed's body.

$$St = \frac{f \cdot L}{V} \tag{6}$$

Where St = Strouhal number $(dimensionless)$, f = vortex frequency (Hz).

3. RESULTS AND DISCUSSION

First, the benchmark results obtained in the present work are compared with different data from the literature in Figure 4. The results obtained in the present work are among the results obtained in the literature, where a good agreement with the available data is observed. The model performed in this work for Reynolds = 15000 compared to experimental models in the literature by Ahmed *et al.* (1984) and Korkischko (2006) showed a difference of only 5.81 %. The model studied in this work for Reynolds = 30000 compared with the numerical model of Bruneau *et al.* (2007), presented a difference of 13.01 %.

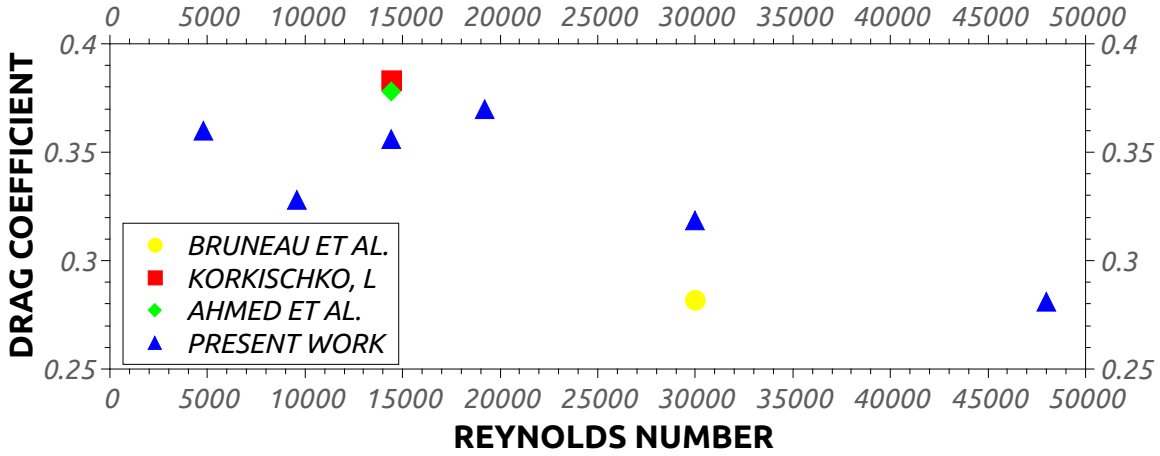

Figure 4. Validation of results

The velocity and pressure fields are presented for seven cases with four different velocities for each case, totaling twenty-eight cases. All of these fields are presented for the instant t = 2 s. For the evaluation of the drag coefficients, a width of 0.01 m was considered, maintaining the proportion of the body on an Ahmed scale. The time below 1s for the transient analysis was disregarded, in order to reduce the coefficient variations, due to its numerical instability. The transient results are seen in Figure 5.

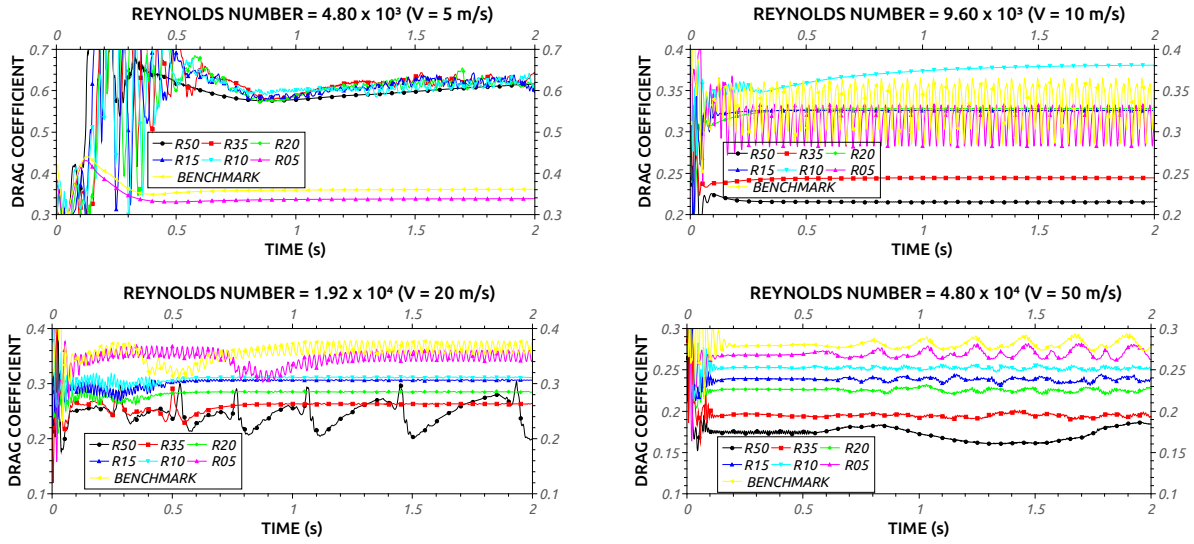

Figure 5. Drag coefficients along time for different Re

For Reynolds number = 4.80 x 10^3 (V = 5 m/s), there are 2 different behaviors, one for the benchmark and R05 and a second behavior for the other geometries. For benchmark and R05, the drag coefficient is around 0.36 and 0.34 respectively, while for the others this coefficient rises to 0.6. As observed in the velocity fields of Figure 5, this increase in C_d is due to the increase in the recirculation zone at the Ahmed's body wake. In these cases, after the detachment of the boundary layer in the frontal region, there was no layer reattachment on the Ahmed top surface and a broad wake as formed. This effect is also evident in the velocity profiles shown in Figure 6, which illustrates the decrease of the velocity magnitude for R10 and above at the positions x = 32 and x = 34, for instance (Figure 7).

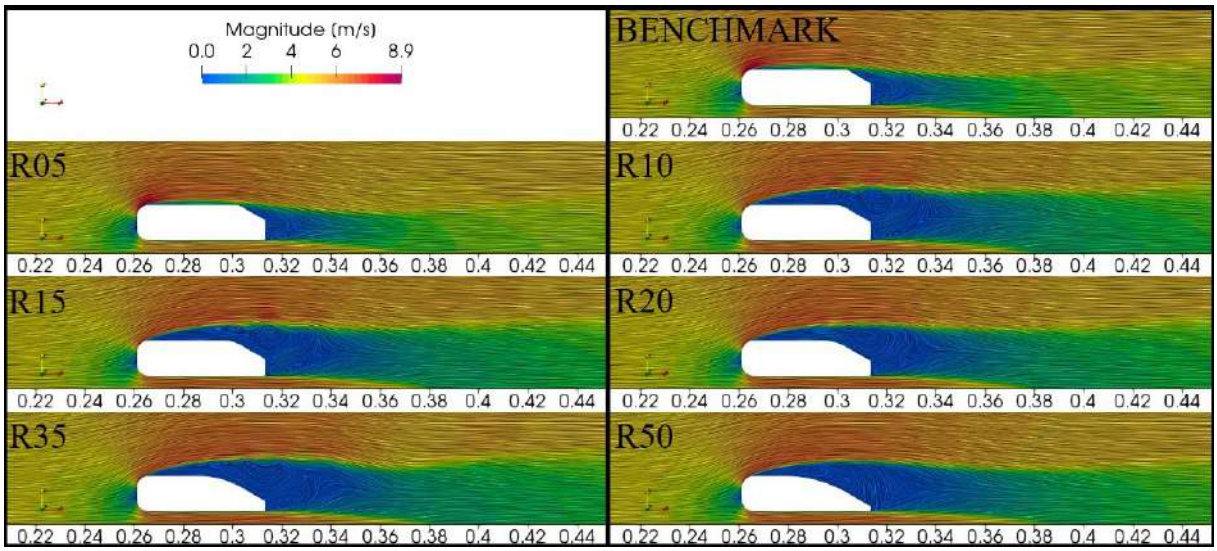

Figure 6. V = 5 m/s for different radius

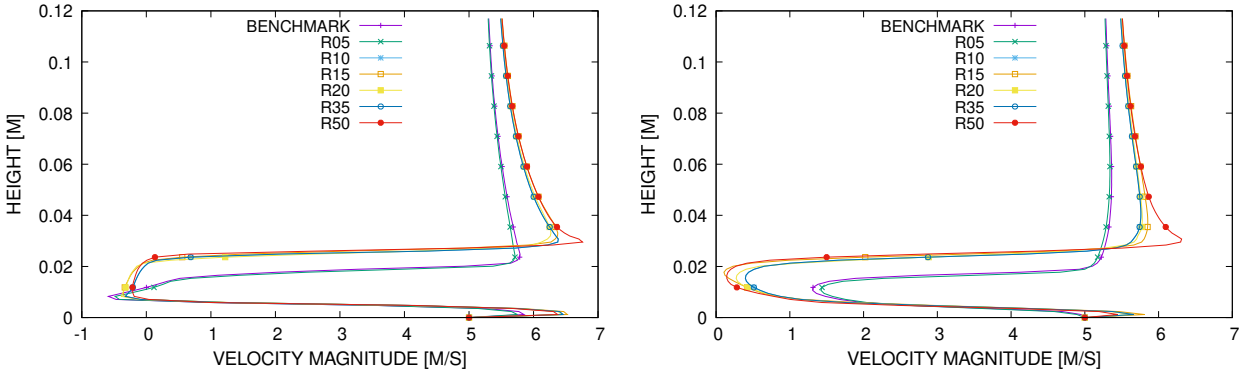

Figure 7. Velocities profiles for the distance of 0.32 and 0.34 respectively

For the Reynolds number = 9.60 x 10^3 (V = 10 m/s), the original radius and R05 were observed in the first cases, oscillations with a small amplitude (f = 0.05 Hz - $St = 0.00104$) of the coefficient along of the entire time span. These peaks are caused by the alternating emission of vortices at the Ahmed's body wake, as shown in Figure 9, which results in this temporal oscillation. Specifically for the R10, due the presence of the recirculation bubble at the top, an increase in C_d is observed, with an average value of 0.375. With the increase of the R15 and R20, the C_d no longer oscillates, presenting a quasi-static behavior ($St = 0$) with a drag coefficient reduction to the average value of 0.328. On the near wake of R10, R15 and R20, two counter-rotating recirculation bubbles are observed, which tend to decrease with increasing radius. With the increase in radius, the reduction of counter-rotating bubbles is noticeable, as shown in R35 and R50 that only a small recirculation zone remains. The recirculation region for these fillet radius has decreased dramatically, consequently the C_d has also decreased.

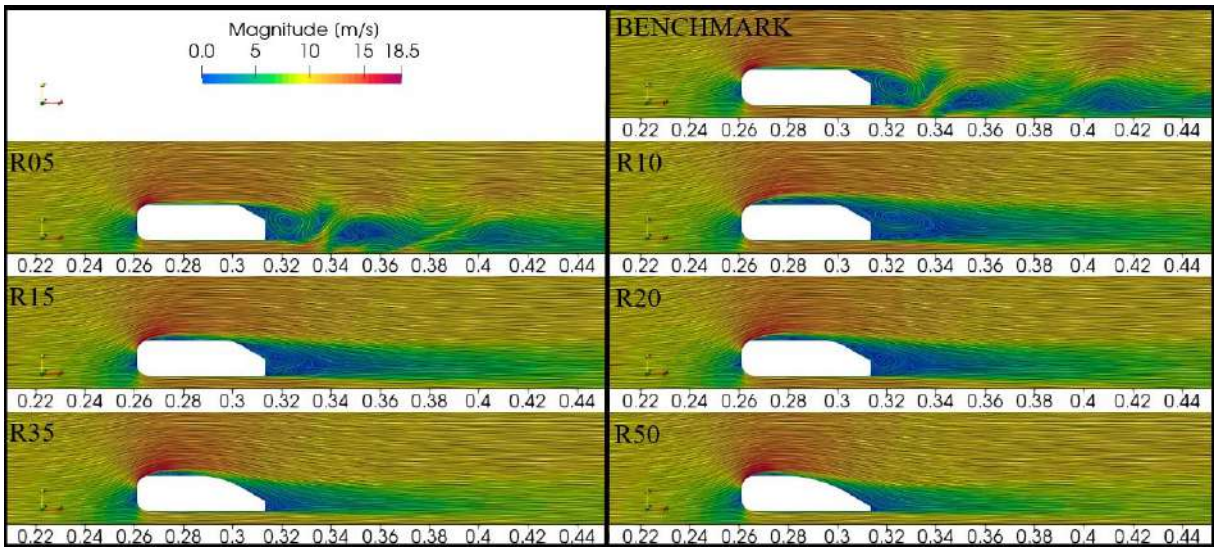

Figure 8. V = 10 m/s for different radius

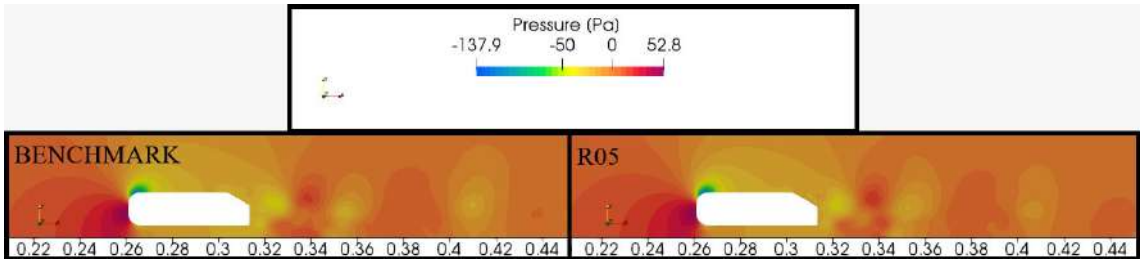

Figure 9. Benchmark pressure and 0.005 m radius with V = 10 m/s

For the Reynolds number = 1.92 x 10^4 (V = 20 m/s), it is observed for the benchmark and R05 oscillations with small amplitude ($f = 0.0235$ Hz, $St = 0.00017$) of the drag coefficient over time. With the increase of the radius to R10, R15, R20 and R35, the C_d no longer oscillates, presenting a quasi-static behavior ($St = 0$) with a drop to the value from 0.26 to 0.315. On the wake, there is the formation of two counter-rotating bubbles that tend to decrease with increasing radius. A new periodicity is perceived for R50 ($f = 0.435$ Hz, $St = 0.0003132$). The recirculation region for these radius decreases and consequently the C_d also decreases. It is also possible to observe that the drag coefficient stops for the larger radius, it is decreased much less in relation to the smaller radius, with the decreased of the velocities.

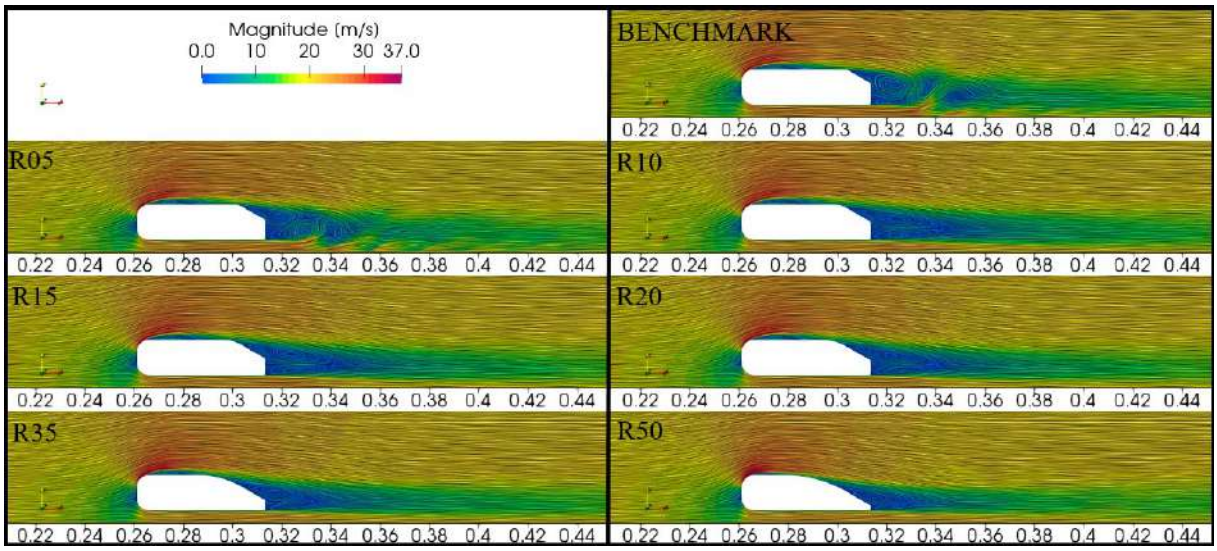

Figure 10. V = 20 m/s for different radius

For the Reynolds number = 4.80 x 10^4 (V = 50 m/s) were observed in the original radius cases, R05, R10, R15, R20 and R35 oscillations with small amplitude ($f = 0.11$ Hz, $St = 0.000316$) of the coefficient over the entire time span.

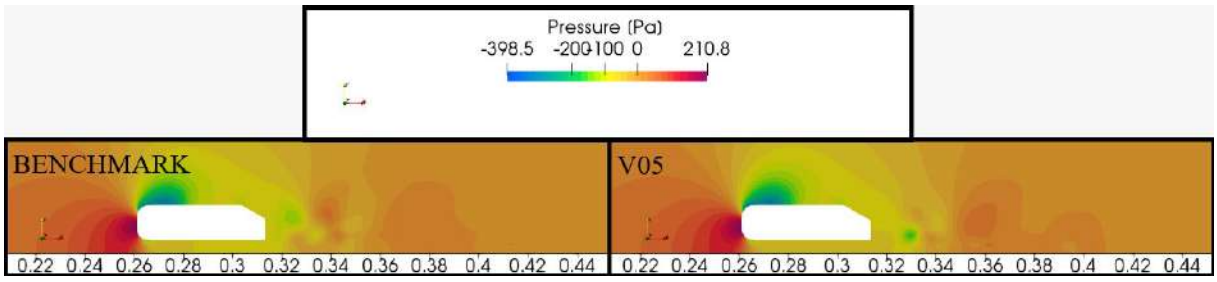

Figure 11. Benchmark pressure and 0.005 m radius with V = 20 m/s

For the final case, R50, there is a stabilization over time. As the fillet radius increases, the drag coefficient decreases accordingly. The flow pattern is the same for all fillet radius. The difference between them is the wake width is reduced as the fillet radius increases.

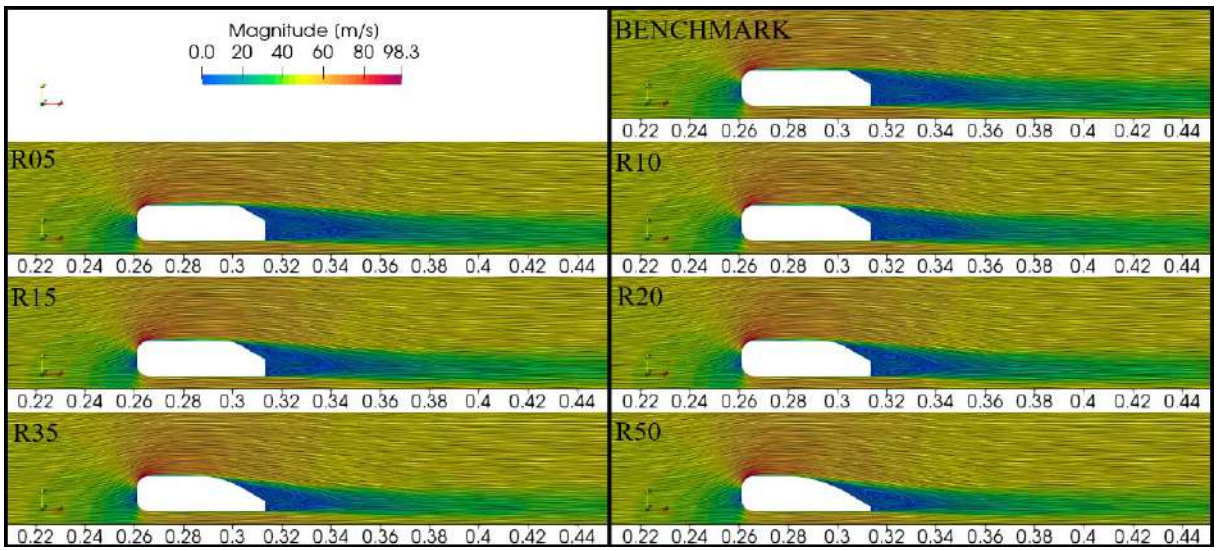

Figure 12. V = 20 m/s for different radius

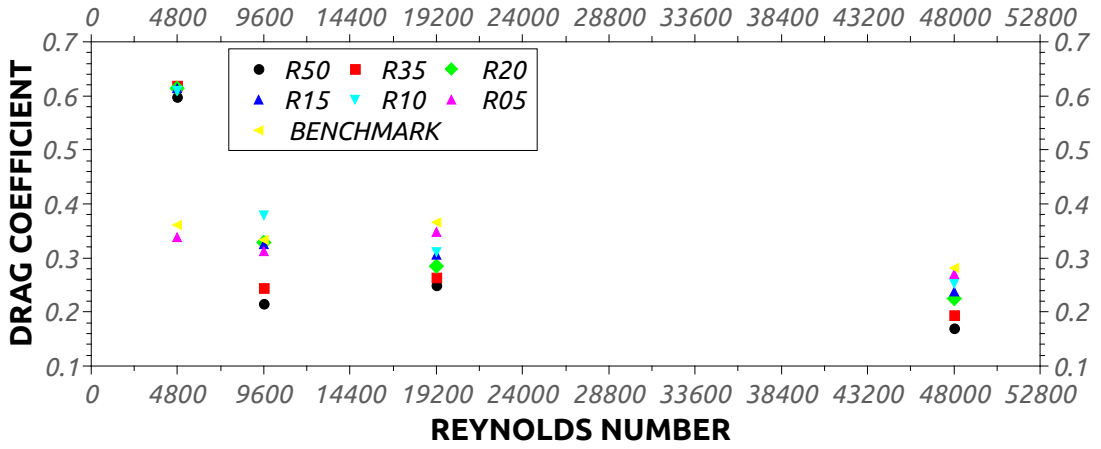

Figure 13. Drag coefficient results

For the drag coefficient, it was possible to observe for the smallest radius with the lowest velocity (5 m/s) studied, the C_d are smaller in relation to the larger radius. With the increase in velocity, the largest radius showed better performance, with the smallest C_d in all cases (10 m/s, 20 m/s and 50 m/s), as seen in the Figure 13. Ahmed's original body showed variations in C_d, decreasing with increasing velocity where it started at 0.38 and ended at 0.28, a reduction of 26.31 %, with velocities of 5 m/s and 50 m/s. The body with the largest radius, 50 mm, presented variations in C_d, decreasing with increasing velocity, where it started at 0.61 and ended at 0.18, a reduction of 70.49 %, with velocities of 5 m/s if 50 m/s.

4. CONCLUSION

We can conclude that the studied models that present the highest efficiency in relation to C_d (smallest coefficient) are the ones with the largest radius for the highest velocities and the ones with the smallest radius for the lowest velocities. It is also possible to observe that Ahmed's original body did not have the smallest C_d in any of the studied cases. This numerical study can also be compared to an everyday situation. A car consumes more fuel in the city compared to the road, one of the reasons that causes this reduction in fuel on the road, is directly linked to this article, where it was possible to observe that in the increase in velocity and Reynolds number, the drag coefficient decreased, decreasing the friction between the flow and the body, consequently reducing fuel consumption.

5. REFERENCES

Ahmed, S.R., Ramm, G. and Faltin, G., 1984. "Some salient features of the time -averaged ground vehicle wake". *SAE International*, Vol. 93, No. 2, pp. 473–503.

Ataídes, R.S.C., 2009. *Implementation of the non linear effects of the Reynolds tensor in turbulence models based on the Boussinesq assumption (in portuguese)*. Master's thesis, Universidade de Brasília, Brasília, Brasil.

Bruneau, C.H., Gilliéron, P. and Mortazavi, I., 2007. "Flow manipulation around the ahmed body with a rear window using passive strategies". *C. R. Mecanique*, Vol. 335, No. 1, pp. 213–218.

Carregari, A.L., 2006. *Air flow study past a bus using CFD and comparing with experimental data (in portuguese)*. Master's thesis, Escola de Engenharia de São Carlos da Universidade de São Paulo, São Carlos, Brasil.

Castejo, D., 2011. *Drag reduction methods and its impact on the vehicle stability (in portuguese)*. Master's thesis, USP São Carlos, São Carlos, Brasil.

Guilmineau, E., Deng, G., Leroyer, A., Queutey, P., Visonneau, M. and Wackers, J., 2018. "Assessment of hybrid ransles formulations for flow simulation around the ahmed body". *Computers Fluids*, Vol. 176, p. 302 – 319.

Korkischko, I., 2006. *Experimental investigation and numerical simulation of the flow around an automobile model: Ahmed's body (in Portuguese)*. Ph.D. thesis, Graduate Program in Mechanical Engineering, Polytechnic School of the University of São Paulo, São Paulo, Brasil.

Krajnovic, S. and Davidson, L., 2005. "Influence of floor motions in wind tunnels on the aerodynamics of road vehicles". *J. Wind Eng. Ind. Aerodyn.*, Vol. 93, No. 9, p. 677–696.

Menter, F.R., Kuntz, M. and Langtry, R., 2003. "Ten years of industrial experience with the sst turbulence model". *In Pro-ceedings of the fourth international symposium on turbulence, heat and mass transfer*, Vol. 4, No. 1, pp. 625–638.

Raina, A., Harmain, G. and Haq, M.I.U., 2017. "Numerical investigation of flow around a 3d bluff body using deflector plate". *International Journal of Mechanical Sciences*, Vol. 131, No. 1, pp. 701–711.

Rocha, S.L., 2016. *Numerical analysis of the external flow field at the Ahmed body for automotive applications (in portuguese)*. Ph.D. thesis, Federal University of Santa Catarina, Santa Catariva, Brasil.

Sousa, S.I., Silva, C.V. and Balestra, G.C., 2010. "Numerical analysis of the flow past a ideal road vehicle: the ahmed body (in portuguese)".

6. RESPONSIBILITY NOTICE

The authors are solely responsible for the printed material included in this paper.